

Model-Independent $\bar{\nu}_e$ Short-Baseline Oscillations from Reactor Spectral Ratios

S. Gariazzo

Instituto de Física Corpuscular (CSIC-Universitat de València), Paterna (Valencia), Spain

C. Giunti

Istituto Nazionale di Fisica Nucleare (INFN), Sezione di Torino, Via P. Giuria 1, I-10125 Torino, Italy

M. Laveder

*Dipartimento di Fisica e Astronomia “Galileo Galilei”,
Università di Padova, Via F. Marzolo 8, I-35131 Padova, Italy and
Istituto Nazionale di Fisica Nucleare (INFN), Sezione di Padova, Via F. Marzolo 8, I-35131 Padova, Italy*

Y.F. Li

*Institute of High Energy Physics, Chinese Academy of Sciences, Beijing 100049, China and
School of Physical Sciences, University of Chinese Academy of Sciences, Beijing 100049, China
(Dated: 16 April 2018)*

We consider the ratio of the spectra measured in the DANSS neutrino experiment at 12.7 and 10.7 m from a nuclear reactor. These data give a new model-independent indication in favor of short-baseline $\bar{\nu}_e$ oscillations which reinforce the model-independent indication found in the late 2016 in the NEOS experiment. The combined analysis of the NEOS and DANSS spectral ratios in the framework of 3+1 active-sterile neutrino mixing favor short-baseline $\bar{\nu}_e$ oscillations with a statistical significance of 3.7σ . The two mixing parameters $\sin^2 2\theta_{ee}$ and Δm_{41}^2 are constrained at 2σ in a narrow- Δm_{41}^2 island at $\Delta m_{41}^2 \simeq 1.3 \text{ eV}^2$, with $\sin^2 2\theta_{ee} = 0.049 \pm 0.023 (2\sigma)$. We discuss the implications of the model-independent NEOS+DANSS analysis for the reactor and Gallium anomalies. The NEOS+DANSS model-independent determination of short-baseline $\bar{\nu}_e$ oscillations allows us to analyze the reactor rates without assumptions on the values of the main reactor antineutrino fluxes and the data of the Gallium source experiments with free detector efficiencies. The corrections to the reactor neutrino fluxes and the Gallium detector efficiencies are obtained from the fit of the data. In particular, we confirm the indication in favor of the need for a recalculation of the ^{235}U reactor antineutrino flux found in previous studies assuming the absence of neutrino oscillations.

I. INTRODUCTION

Neutrino oscillations revealed the existence of neutrino masses and are one of the most powerful tools in the search of new physics beyond the Standard Model. An interesting indication of new physics is given by the reactor [1] and Gallium [2–8] short-baseline neutrino oscillation anomalies, which can be explained by the existence of a non-standard sterile neutrino at the eV mass scale (see the recent fits in Refs. [9, 10]).

The reactor antineutrino anomaly [1] was discovered in 2011 as a consequence of a new calculation of the reactor $\bar{\nu}_e$ fluxes [11, 12] due to the fissions of ^{235}U , ^{238}U , ^{239}Pu , and ^{241}Pu . The predicted total rates of $\bar{\nu}_e$ detection were found to be a few percent larger than those obtained in previous calculations [13–15]. The comparison of the new predicted rates with the rates measured in several experiments at distances between a few meters and about 500 meters from a reactor indicate a deficit of about 5% which can be explained by the disappearance of $\bar{\nu}_e$ during their propagation from the reactor to the detector, that is most likely due to active-sterile neutrino oscillations (see the review in Ref. [16]). However, the correctness of the $\bar{\nu}_e$ flux calculation has been put into question (see Refs. [17, 18]) by the discovery of the so-called “5 MeV bump” of the reactor antineutrino spectrum measured in

the RENO [19, 20], Double Chooz [21], Daya Bay [22], and NEOS [23] experiments. Moreover, the Daya Bay measurement [24] of the correlation between the reactor fuel evolution and the antineutrino detection rate indicates that at least the calculation of the ^{235}U reactor antineutrino flux must be revised [24–27] (see also the recent review in Ref. [28]).

The Gallium neutrino anomaly [2–8] is a deficit of ν_e events measured in the Gallium radioactive source experiments GALLEX [29–31] and SAGE [2, 32–34]. As explained in Ref. [8], in the calculation of the Gallium anomaly the uncertainties of the neutrino-nucleus cross section are taken into account using the $^{71}\text{Ga}(^3\text{He}, ^3\text{H})^{71}\text{Ge}$ measurement in Ref. [35]. However, the efficiencies of the GALLEX and SAGE detectors are not known and could have been overestimated.

In this paper we consider the new results of the DANSS reactor neutrino experiment presented in Ref. [36]¹. We will show that the ratio of the spectra measured in the DANSS experiment at 12.7 and 10.7 m from a nuclear reactor provide a model-independent indication of short-baseline $\bar{\nu}_e$ oscillations which reinforces the model-

¹ The same results have been published in arXiv:1804.04046 after completion of this work.

independent indication found in the late 2016 in the NEOS experiment [23].

We will show that the combined analysis of the NEOS and DANSS spectral ratios allow us to determine the neutrino mixing parameters in a model-independent way. In particular, the determination of neutrino oscillations is independent from the reactor anomaly, which depends on the comparison of the measured and calculated reactor rates [11, 12], and from the Gallium anomaly, which depends on the estimated efficiencies of the GALLEX and SAGE detectors. This is a remarkable result that raises to a new level the significance of the indications in favor of short-baseline ν_e and $\bar{\nu}_e$ disappearance.

Moreover, the NEOS+DANSS model-independent determination of the neutrino oscillation parameters allow us to derive the values of the ^{235}U , ^{238}U , and ^{239}Pu reactor antineutrino fluxes which are needed to fit the reactor rates and the Daya Bay evolution data [24] and the efficiencies of the GALLEX and SAGE detectors that are needed to explain the Gallium anomaly.

We work in the 3+1 framework explained in Ref. [16], which is a perturbation of the standard three-neutrino mixing framework which explains the oscillations observed in solar, atmospheric and long-baseline neutrino experiments (see Refs. [37–39]). We use the notation of Ref. [9], of which we only remind that short-baseline oscillations depend on the squared-mass difference Δm_{41}^2 and the amplitude of ν_e and $\bar{\nu}_e$ disappearance can be parameterized by the effective mixing angle ϑ_{ee} given by

$$\sin^2 2\vartheta_{ee} = 4|U_{e4}|^2 (1 - |U_{e4}|^2), \quad (1)$$

U is the 4×4 unitary mixing matrix [40]. Sometimes ϑ_{ee} is called ϑ_{14} (see, for example, Ref. [10]).

In this paper we consider only short-baseline ν_e and $\bar{\nu}_e$ disappearance experiments. In particular we do not consider the LSND anomaly [41, 42], which is a signal of short-baseline $\bar{\nu}_\mu \rightarrow \bar{\nu}_e$ appearance which can be explained in the framework of 3+1 active sterile neutrino mixing (see Ref. [16]). However, the strong limits on $\langle \bar{\nu}_\mu \rangle$ disappearance obtained recently in the MINOS and MINOS+ experiments [43] increase to an unacceptable level the appearance-disappearance tension discussed in many papers [9, 10, 16, 40, 44–53]. Indeed, adding the MINOS and MINOS+ data to the data considered in our PrGlo17 fit [9], we obtain an appearance-disappearance parameter goodness-of-fit of about 0.4%². This result disfavors the LSND anomaly, but a definitive conclusion on the LSND

² In this analysis we used the public MINOS and MINOS+ code [43] which relies on the neutrino flux prediction of the MINERvA collaboration [54]. With a “shape analysis” of the MINOS and MINOS+ data allowing different free normalizations for the predictions of the charged-current and neutral-current events, we obtained an appearance-disappearance parameter goodness-of-fit of about 0.5%, which is still too small. The details of these analyses will be presented elsewhere.

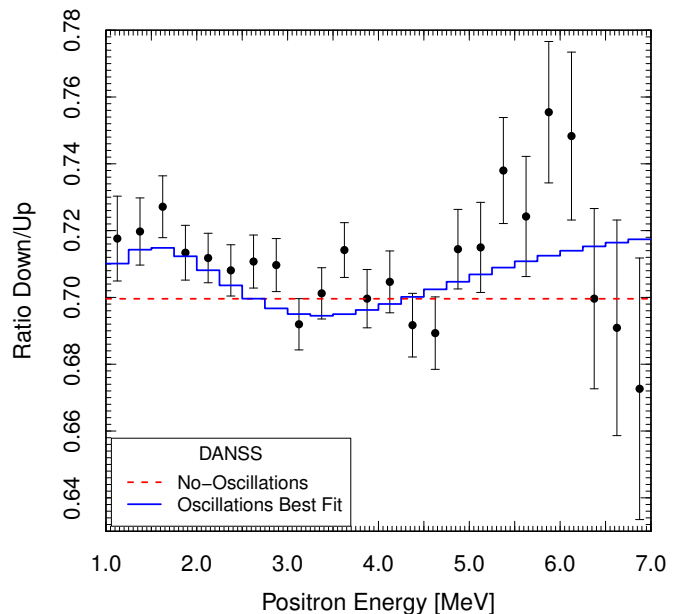


FIG. 1. The Down/Up DANSS spectral data presented in Ref. [36]. The red dashed line shows the best-fit of the data without oscillations and a free normalization. The blue solid line shows the best-fit that we obtained with neutrino oscillations and a free normalization.

$\bar{\nu}_\mu \rightarrow \bar{\nu}_e$ signal will be possible only after its direct test in the SBN [55] and JSNS² [56] experiments.

The plan of the paper is as follows. In Section II we present our analysis of DANSS data and the results of the NEOS+DANSS combined fit. In Section III we compare the results of the NEOS+DANSS fit with the reactor and Gallium anomalies. In Section IV we present the results of a model-independent fit of short-baseline ν_e and $\bar{\nu}_e$ disappearance data. Finally, we draw our conclusions in Section V.

II. DANSS AND NEOS

DANSS is a neutrino experiment with a solid scintillator detector located under a commercial power reactor which emits a huge $\bar{\nu}_e$ flux leading to a high-statistics measurement. The DANSS detector is installed on a movable platform which allows to change the distance between the centers of the reactor and detector from 10.7 to 12.7 m. We analyzed the Down/Up DANSS data presented in Ref. [36] on the ratio of the energy spectra measured at the two distances.

As reported in Ref. [36], the DANSS collaboration found that the best fit of the Down/Up spectral ratio is obtained for short-baseline neutrino oscillations with a χ^2 that is smaller by 13.3 with respect to the case of no oscillations. They found the best fit at $\sin^2 2\vartheta_{ee} = 0.045$ and $\Delta m_{41}^2 = 1.4 \text{ eV}^2$.

The DANSS data are shown in Fig. 1. In our analysis, for each energy bin we averaged the oscillation probabil-

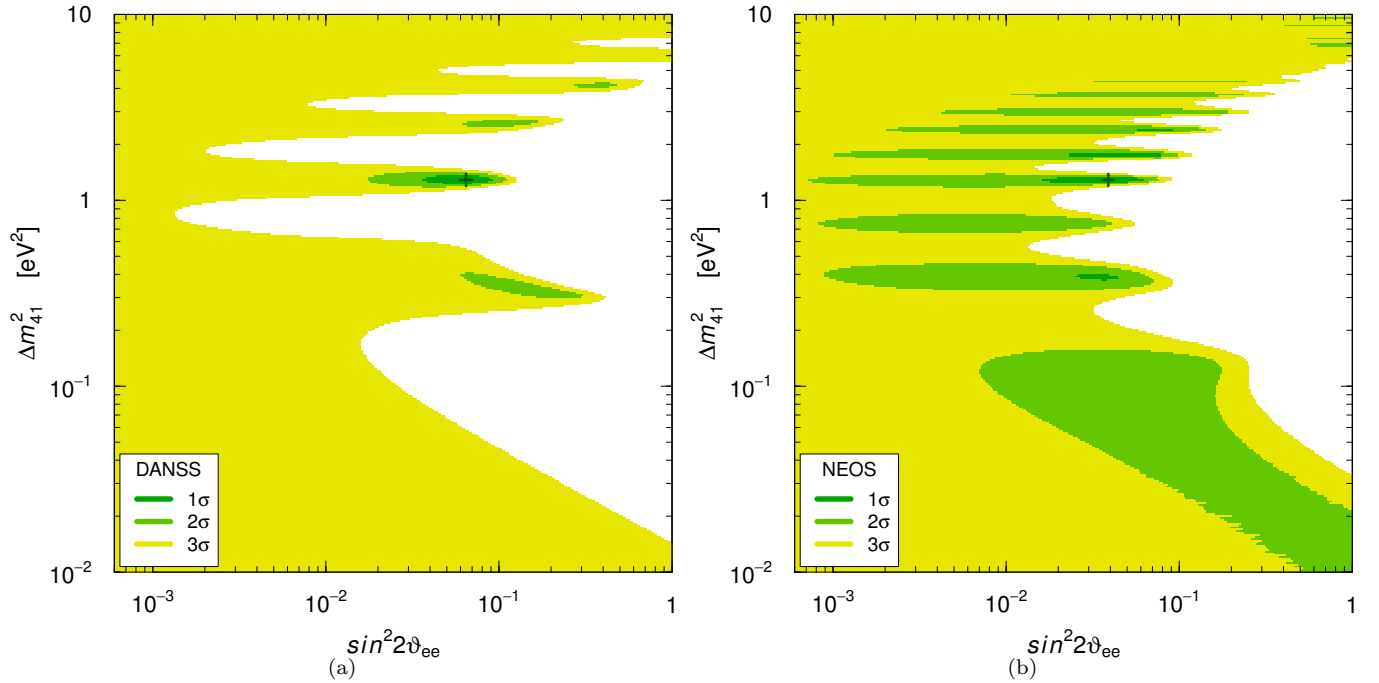


FIG. 2. Allowed regions in the $\sin^2 2\theta_{ee}-\Delta m_{41}^2$ plane obtained from the fits of (a) DANSS [36] and (b) NEOS [23] data. The best-fit points corresponding to the χ_{\min}^2 in Table I are indicated by crosses.

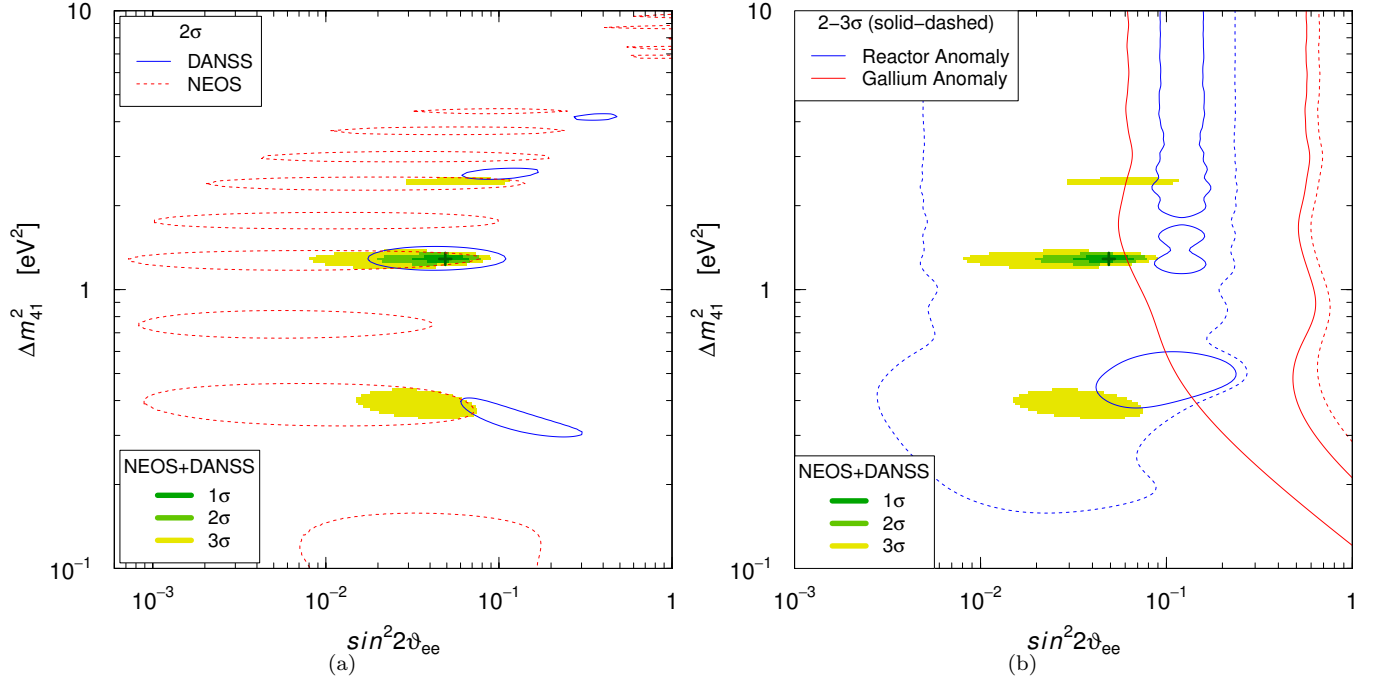


FIG. 3. Allowed regions in the $\sin^2 2\theta_{ee}-\Delta m_{41}^2$ plane obtained from the combined fit of the data of the DANSS [36] and NEOS [23] experiments (shaded regions). (a) Comparison of the allowed regions with the 2σ allowed regions of DANSS and NEOS. (b) Comparison of the allowed regions with the regions allowed at 2 and 3σ by the reactor anomaly and by the Gallium anomaly.

ity over the geometrical volumes of the reactor and the detector. We allowed a free normalization of the data and

we took into account the 25% energy resolution reported in Ref. [36] and a correlated 2% systematic uncertainty

(following Ref. [10]). We obtained a χ^2 that is smaller by 11.4 with respect to the case of no oscillations and the best fit at $\sin^2 2\vartheta_{ee} = 0.065$ and $\Delta m_{41}^2 = 1.3 \text{ eV}^2$. These results are in an acceptable approximate agreement with those obtained by the DANSS collaboration in Ref. [36] and slightly more conservative.

Figure 2(a) shows the allowed regions in the $\sin^2 2\vartheta_{ee} - \Delta m_{41}^2$ plane obtained from our analysis of the data of the DANSS experiment. It is interesting to compare them with the allowed regions obtained from the analysis of the NEOS experiment [23] shown in Fig. 2(b). One can see that there is a remarkable agreement between the DANSS and NEOS best-fit regions which lie in a narrow interval around $\Delta m_{41}^2 \simeq 1.3 \text{ eV}^2$ with compatible values of $\sin^2 2\vartheta_{ee}$.

Let us emphasize that these indications in favor of short-baseline neutrino oscillations are model-independent, because they depend only on measured spectral ratios: the Down/Up spectral ratio for DANSS [36] and the NEOS/Daya Bay spectral ratio for NEOS [23] (the NEOS spectrum measured at a distance of 24 m was normalized to the Daya Bay spectrum [22] measured at the large distance of about 550 m, where short-baseline oscillations are averaged out). In particular, these indications do not depend on the calculation of the reactor $\bar{\nu}_e$ fluxes on which the reactor antineutrino anomaly is based [1].

The statistical significance of the NEOS+DANSS indication in favor of short-baseline $\bar{\nu}_e$ oscillations is of 3.7σ . This value is similar to the statistical significance of the reactor and Gallium anomalies that we found in Ref. [9]. However, it is much more reliable, because it is model-independent.

Figure 3(a) shows the results of the combined fit of the DANSS and NEOS data, together with the 2σ allowed regions of DANSS and NEOS. One can see that there is a good overlap of the DANSS and NEOS allowed regions at $\Delta m_{41}^2 \simeq 1.3 \text{ eV}^2$, which determines the region preferred by the combined fit, with the best-fit oscillation parameters in Table I. There are also small overlaps of the DANSS and NEOS allowed regions at $\Delta m_{41}^2 \simeq 0.4 \text{ eV}^2$ and $\Delta m_{41}^2 \simeq 2.5 \text{ eV}^2$ that determine two narrow islands allowed at 3σ by the combined fit.

III. THE REACTOR AND GALLIUM ANOMALIES

As emphasized in the Section II, the DANSS and NEOS spectral ratios give indications of short-baseline $\bar{\nu}_e$ oscillations which are independent of the reactor flux calculation. This indication is much more robust than those of the reactor and Gallium anomalies, which suffer from the dependence on the calculated reactor fluxes and the assumed Gallium detector efficiencies. Figure 3(b) shows the comparison of the NEOS+DANSS allowed regions in the $\sin^2 2\vartheta_{ee} - \Delta m_{41}^2$ plane with the 2 and 3σ allowed regions of the reactor and Gallium anomalies from Ref. [9].

	NEOS+DANSS	MI ν_e Dis 235+239	MI ν_e Dis 235+238+239
χ_{\min}^2	81.0	138.5	136.5
NDF	81	144	143
GoF	48%	61%	64%
Δm_{41}^2	1.29 ± 0.03	1.29 ± 0.03	1.29 ± 0.03
$\sin^2 2\vartheta_{ee}$	0.049 ± 0.011	$0.047^{+0.009}_{-0.011}$	$0.043^{+0.014}_{-0.009}$
r_{235}	—	0.957 ± 0.011	$0.970^{+0.015}_{-0.013}$
r_{238}	—	—	$0.76^{+0.15}_{-0.16}$
r_{239}	—	$1.005^{+0.034}_{-0.032}$	$1.056^{+0.062}_{-0.042}$
η_G	—	$0.869^{+0.080}_{-0.062}$	$0.863^{+0.087}_{-0.061}$
η_S	—	$0.836^{+0.075}_{-0.057}$	$0.854^{+0.060}_{-0.075}$
$ U_{e4} ^2$	0.012 ± 0.003	$0.012^{+0.002}_{-0.003}$	$0.011^{+0.003}_{-0.002}$
$\sigma_{f,235}$	—	6.40 ± 0.07	$6.49^{+0.10}_{-0.09}$
$\sigma_{f,238}$	—	—	$7.6^{+1.5}_{-1.6}$
$\sigma_{f,239}$	—	$4.42^{+0.15}_{-0.14}$	$4.65^{+0.27}_{-0.18}$
$\Delta\chi_{\text{NO}}^2$	16.7	14.9	14.6
$n\sigma_{\text{NO}}$	3.7	3.4	3.4

TABLE I. Results of the fits of ν_e and $\bar{\nu}_e$ disappearance data: minimum χ^2 (χ_{\min}^2), number of degrees of freedom (NDF), goodness of fit (GoF): best fit values of Δm_{41}^2 , $\sin^2 2\vartheta_{ee}$, r_{235} , r_{238} , r_{239} , η_G , η_S , and those of the derived quantities $|U_{e4}|^2$, $\sigma_{f,235}$, $\sigma_{f,238}$, $\sigma_{f,239}$; χ^2 difference $\Delta\chi_{\text{NO}}^2$ between the χ^2 of no oscillations and χ_{\min}^2 , and the resulting number of σ 's ($n\sigma_{\text{NO}}$) for two degrees of freedom corresponding to two fitted oscillation parameters ($\sin^2 2\vartheta_{ee}$ and Δm_{41}^2). The cross sections per fission $\sigma_{f,i}$ are expressed in units of $10^{-43} \text{ cm}^2/\text{fission}$.

From Fig. 3(b) one can see that the NEOS+DANSS model-independent allowed regions are compatible with the 3σ allowed regions of the reactor anomaly, but have some tension with the 2σ allowed regions. The tension can be quantified by the parameter goodness of fit [57], whose value is 2% ($\Delta\chi^2/\text{NDF} = 8.0/2$). Hence our model-independent analysis indicate that the reactor anomaly overestimates the $\bar{\nu}_e$ disappearance. This is probably due to an overestimate of the reactor antineutrino fluxes. In Section IV we will obtain from the combined model-independent fit the needed corrections to the values of the reactor antineutrino fluxes.

Figure 3(b) also shows that there is a compatibility of the 3σ regions allowed by the NEOS+DANSS model-independent results with those allowed by the Gallium anomaly, while there is a tension of the 2σ allowed regions, corresponding to a parameter goodness of fit of 4% ($\Delta\chi^2/\text{NDF} = 6.6/2$). This tension suggests that the efficiencies of the GALLEX and SAGE detectors may have been overestimated. In the combined model-independent fit presented in Section IV we will obtain an estimate of the needed corrections to those efficiencies.

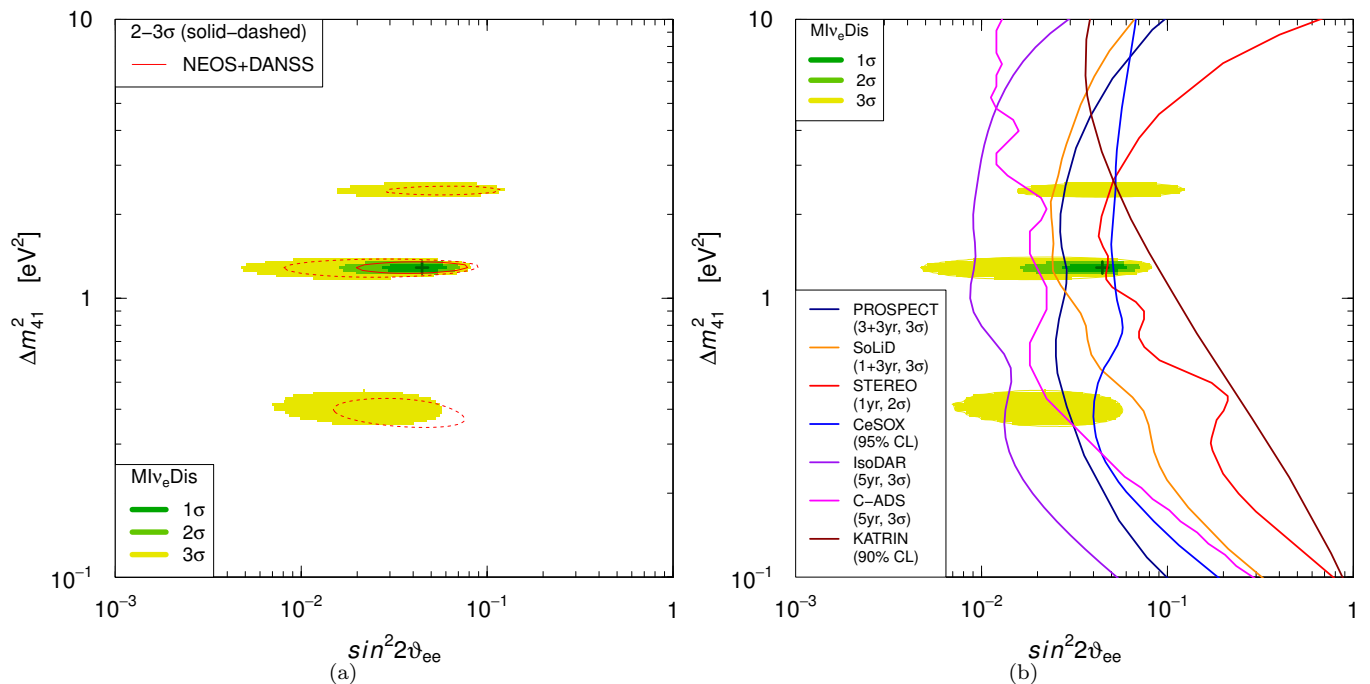


FIG. 4. Allowed regions in the $\sin^2 2\theta_{ee} - \Delta m_{41}^2$ plane obtained from the fits of model-independent short-baseline ν_e and $\bar{\nu}_e$ disappearance data (Ml ν_e Dis). (a) Comparison with the regions allowed at 2 and 3 σ by the NEOS and DANSS data (same as in Fig. 3). (b) Comparison with the sensitivities of future experiments.

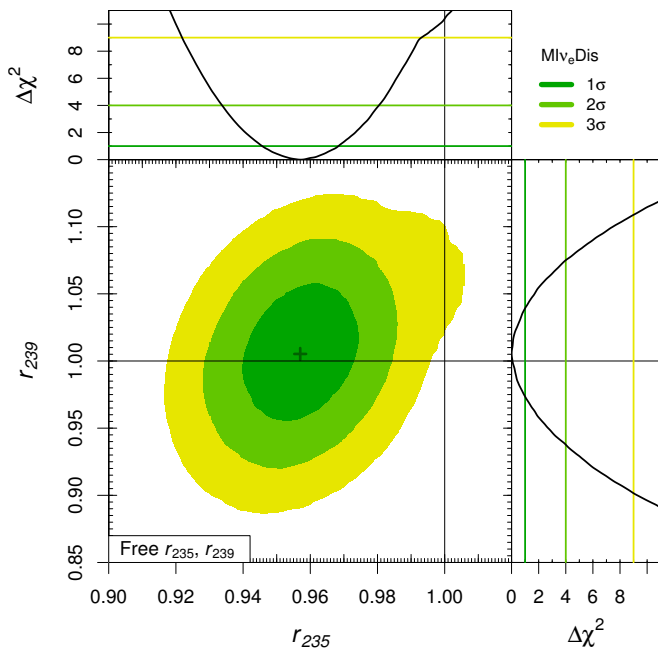


FIG. 5. Allowed regions in the $r_{235} - r_{239}$ plane and marginal $\Delta\chi^2$'s obtained from the fit of model-independent short-baseline ν_e and $\bar{\nu}_e$ disappearance data with free r_{235} and r_{239} . The best-fit points corresponding to the χ_{\min}^2 in Table I are indicated by crosses.

IV. MODEL-INDEPENDENT ν_e AND $\bar{\nu}_e$ DISAPPEARANCE

As discussed in the Section II, the combined fit of the DANSS and NEOS spectral ratios give a model-independent indication in favor of short-baseline $\bar{\nu}_e$ oscillations. In particular, it is independent of the reactor and Gallium anomalies, which depend, respectively, on the reactor antineutrino flux calculation and on the assumed efficiencies of the Gallium detectors. In this section we present the results of a model-independent analysis of short-baseline ν_e and $\bar{\nu}_e$ disappearance data (Ml ν_e Dis). We considered the DANSS and NEOS spectral ratios, the reactor rates keeping the main reactor antineutrino fluxes as free and the Gallium data with free efficiencies of the GALLEX and SAGE detectors. For completeness, we considered also the following data which constrain neutrino oscillations in a model-independent way and which were included in our previous analyses [8, 9, 16, 53, 58] of ν_e and $\bar{\nu}_e$ disappearance:

- The ratio of the spectra measured at 40 m and 15 m from the source in the Bugey-3 experiment [59].
- The ratio of the KARMEN [60] and LSND [61] $\nu_e + {}^{12}\text{C} \rightarrow {}^{12}\text{N}_{\text{g.s.}} + e^-$ scattering data at 18 m and 30 m from the source [48, 62]

Let us however clarify that the contribution of these data is very small and the results are almost independent of their inclusion in the fit.

Concerning the fit of the reactor rates, we considered the Daya Bay fuel evolution data [24] and the rates of the following experiments (see Table 1 of Ref. [9]): Bugey-4 [63], Rovno91 [64], Bugey-3 [59], Gosgen [65], ILL [66, 67], Krasnoyarsk87 [68], Krasnoyarsk94 [69, 70], Rovno88 [71], SRP [72], Nucifer [73], Chooz [74], Palo Verde [75], RENO [76], and Double Chooz [77]. We improved the analysis of the reactor rates presented in Ref. [26] by taking into account the uncertainties of the reactor fission fractions. For each experimental data point labeled with the index a , we considered the theoretical cross section per fission (that quantifies the $\bar{\nu}_e$ detection rate)

$$\sigma_{f,a}^{\text{th}} = \sum_i f_i^a \bar{F}_i^a r_i \sigma_{f,i}^{\text{SH}}, \quad (2)$$

where $i = 235, 238, 239, 241$ and $\sigma_{f,i}^{\text{SH}}$ are the corresponding theoretical Saclay+Huber cross sections per fission [1, 11, 12]. The average values \bar{F}_i^a of the effective fission fractions are multiplied by the coefficients f_i^a in order to take into account their uncertainties. The coefficients r_i allow us to consider a variation of the $\bar{\nu}_e$ fluxes with respect to the calculated ones. We considered the following two cases:

235+239: Free r_{235} and r_{239} to be determined by the fit.

235+238+239: Free r_{235} , r_{238} , and r_{239} to be determined by the fit.

The case 235+239 is motivated by the fact that the Daya Bay evolution data and the fuel composition of the other reactor experiments constrain mainly the two major ^{235}U and ^{239}Pu fluxes [24–27]. The case 235+238+239 is motivated by the discovery in Ref. [27] that also the ^{238}U flux can be loosely constrained. On the other hand, the ^{241}Pu flux is not constrained at all, as we have verified through a tentative analysis with all r_i free.

We analyzed the reactor rates with the least-squares statistic

$$\begin{aligned} \chi^2 = & \sum_{a,b} \left(P_{ee}^a \sum_i f_i^a \bar{F}_i^a r_i \sigma_{f,i}^{\text{SH}} - \sigma_{f,a}^{\text{exp}} \right) (V_{\text{exp}}^{-1})_{ab} \\ & \times \left(P_{ee}^b \sum_j f_j^b \bar{F}_j^b r_j \sigma_{f,j}^{\text{SH}} - \sigma_{f,b}^{\text{exp}} \right) \\ & + \sum_{i,j \in \Omega} (r_i - 1) (V_{\text{SH}}^{-1})_{ij} (r_j - 1) \\ & + \sum_{a,b} \sum_{i,j} \left(\frac{f_i^a - 1}{\delta_i^a} \right) (C_{\text{exp}}^{-1})_{ab} (C_f^{-1})_{ij} \left(\frac{f_j^b - 1}{\delta_j^b} \right) \\ & + \sum_a \lambda_a \left[1 - \sum_i f_i^a \bar{F}_i^a \right], \quad (3) \end{aligned}$$

where P_{ee}^a are the $\bar{\nu}_e$ survival probabilities, $\sigma_{f,a}^{\text{exp}}$ are the measured cross sections per fission, V_{exp} is the experimental covariance matrix, V_{SH} is the covariance matrix

of the fractional uncertainties of the Saclay-Huber theoretical calculation of the antineutrino fluxes from the four fissionable nuclides, δ_i^a is the uncertainty of the fission fraction i in the experiment a , C_{exp} is the correlation matrix of the fission fractions in the different experiments and C_f is the correlation matrix of the four fission fractions. In the second sum $\Omega = \{238, 241\}$ in the 235+239 analysis and $\Omega = \{241\}$ in the 235+238+239 analysis. The coefficients λ_a are Lagrange multipliers that enforce the constraint

$$\sum_i f_i^a \bar{F}_i^a = \sum_i \bar{F}_i^a = 1. \quad (4)$$

For experiments at commercial reactors we assumed the value of the fission fraction uncertainty estimated by the Daya Bay collaboration [22], $\delta_i^a = 5\%$, neglecting possible differences on which there is no information. On the other hand, the fission fractions of experiments with research reactors have smaller uncertainties. We found information on the fission fraction uncertainty only for the Nucifer experiment [73], where it was estimated to be 2%. In this experiment the enrichment in ^{235}U was only 19.75%. In the other experiments with research reactors the uncertainty of the fission fractions should be smaller, because the fuel is highly enriched in ^{235}U . Therefore, for them we assumed $\delta_i^a = 1\%$. The correlation matrix C_{exp} correlates the uncertainty of the fission fraction of experiments at the same reactor, for which we assumed 100% correlation. For C_f we used the correlation matrix estimated by the Daya Bay collaboration in Table 2 of Ref. [22].

The results of the 235+239 and 235+238+239 fits are given in Table I. The results for the oscillation parameters $\sin^2 2\vartheta_{ee}$ and Δm_{41}^2 are practically equal in the two analyses. The allowed regions in the $\sin^2 2\vartheta_{ee} - \Delta m_{41}^2$ plane are shown in Fig. 4. In Fig. 4(a) they are confronted with the regions allowed at 2 and 3 σ by the combined analysis of the NEOS and DANSS data (shown already in Fig. 3). One can see that the global model-independent allowed regions are mostly determined by the NEOS and DANSS spectral data, with small effects of the other constraints. Indeed, as one can see from the values in Table I, the statistical significance of short-baseline neutrino oscillations obtained in the $\text{MI}\nu_e\text{Dis}$ analyses is almost the same as that obtained in the NEOS+DANSS analysis, with a slight decrease due to the inclusion of 67 data points that are less constraining than the NEOS and DANSS data.

Figure 4(b) shows the comparison of the allowed regions in the $\sin^2 2\vartheta_{ee} - \Delta m_{41}^2$ plane with the sensitivities of the reactor experiments PROSPECT [78], SoLid [79], STEREO [80], which are under way, of the future experiments CeSOX [81] and KATRIN [82] and of the proposed experiments IsoDAR@KamLAND [83] and C-ADS [84]. One can see that the sensitivities of the reactor experiments cover most of the allowed region. Hence, they have a good chance to confirm the NEOS+DANSS indication if it is correct. The CeSOX experiment is sensitive to the large- $\sin^2 2\vartheta_{ee}$ parts of the allowed regions and the

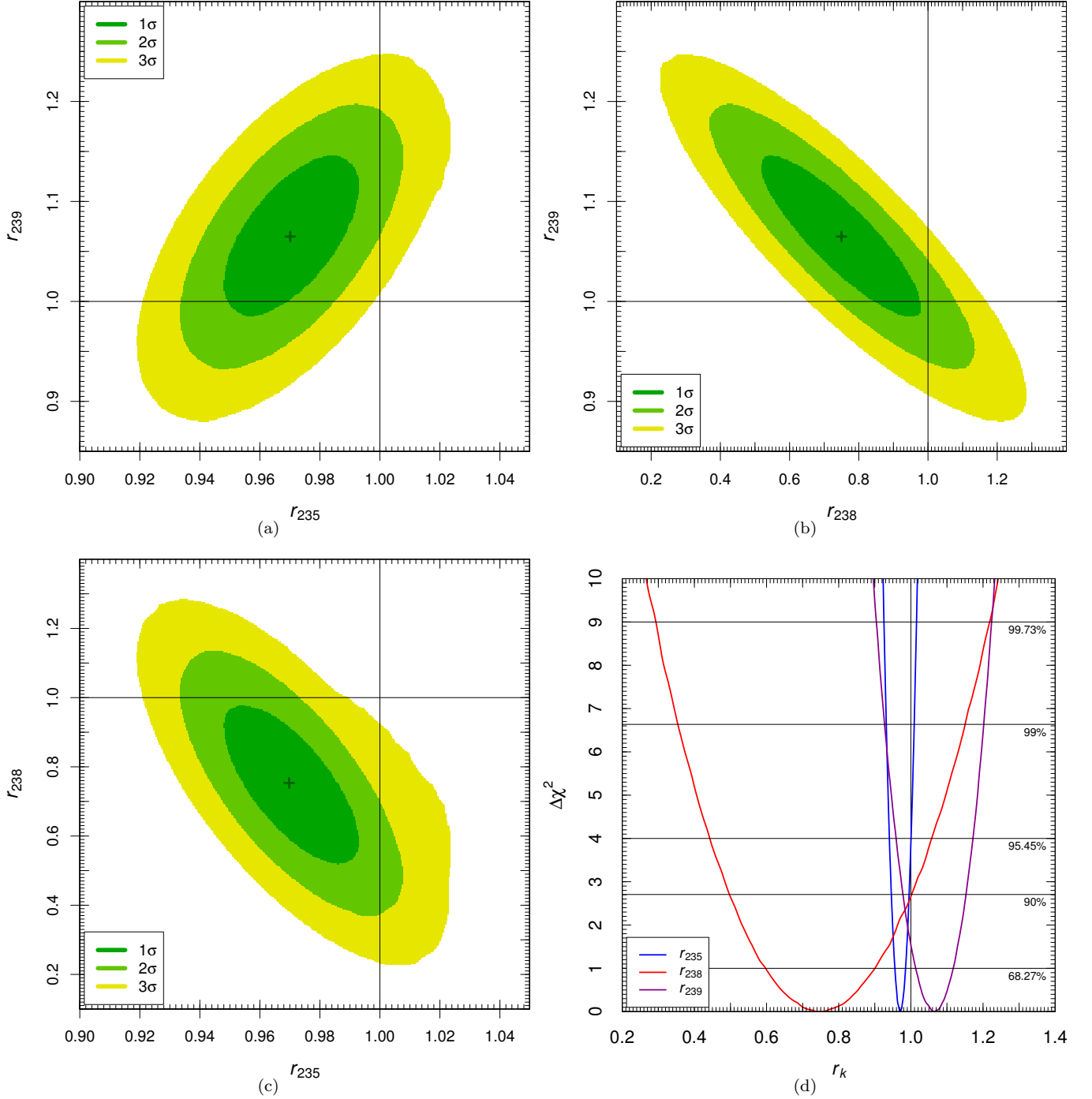


FIG. 6. Allowed regions in the r_{235} - r_{239} , r_{238} - r_{239} , and r_{235} - r_{238} planes and marginal $\Delta\chi^2$'s obtained from the fits of all short-baseline ν_e and $\bar{\nu}_e$ disappearance data with free r_{235} , r_{238} and r_{239} . The best-fit points corresponding to the χ^2_{\min} in Table I are indicated by crosses.

KATRIN experiment is sensitive to the large- $\sin^2 2\vartheta_{ee}$ part of the 3σ allowed region at $\Delta m_{41}^2 \simeq 0.4 \text{ eV}^2$. Also the proposed C-ADS experiment can cover the large- $\sin^2 2\vartheta_{ee}$ parts of the allowed regions. A definitive confirmation or exclusion of the NEOS+DANSS indication may come from the proposed IsoDAR@KamLAND ex-

periment, which covers almost all the 3σ allowed regions.

As explained in Section III the model-independent analysis of the NEOS and DANSS data indicate that the reactor anomaly overestimates the $\bar{\nu}_e$ disappearance. In the 235+239 analysis the reactor anomaly is reduced through the reduction of the ^{235}U antineutrino

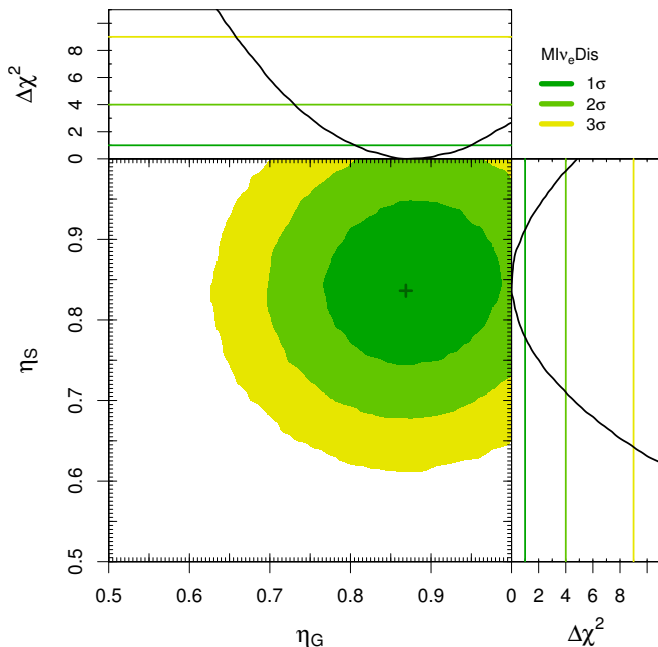


FIG. 7. Allowed regions in the η_G - η_S plane and marginal $\Delta\chi^2$'s obtained from the fit of model-independent short-baseline ν_e and $\bar{\nu}_e$ disappearance data. η_G and η_S are, respectively, the corrections to the efficiencies of the GALLEX and SAGE Gallium detectors. The best-fit points corresponding to the χ^2_{\min} in Table I are indicated by crosses.

flux shown by the best-fit values of r_{235} in Table I. In the 235+238+239 analysis also r_{238} is smaller than one, but its effect is marginal because the contribution of ^{238}U to the total antineutrino flux is only about 8% for commercial power reactors and zero for research reactors.

Figure 5 shows the allowed regions in the r_{235} - r_{239} plane and the marginal $\Delta\chi^2$'s obtained in the 235+239 analysis with free r_{235} and r_{239} . The correlated allowed region in the r_{235} - r_{239} plane has an ellipsoidal shape, except for a bulge at 3σ for large values of r_{235} and r_{239} . The bulge is due to the 3σ allowed region at $\Delta m_{41}^2 \simeq 2.5 \text{ eV}^2$ in Fig. 4, where $\sin^2 2\vartheta_{ee}$ is relatively large and large values of r_{235} and r_{239} are required to compensate the corresponding small $\bar{\nu}_e$ survival probability. From Fig. 5 and the best-fit values of r_{235} - r_{239} in Table I, we conclude that the indication in favor of the need for a recalculation of $\sigma_{f,235}$ already found in Refs. [24–27] is confirmed. The value of $\sigma_{f,235}$ in Table I is compatible, within the uncertainties, with that found in Refs. [24–27] assuming the absence of neutrino oscillations. This is a remarkable result and we want to emphasize that it depends on the stronger constraints on the allowed oscillation parameters due to the DANSS and NEOS spectral ratios. Indeed, the value of $\sigma_{f,235}$ that was found in Ref. [26] with a fit of the reactor rates using a free r_{235} and allowing neutrino oscillations is $r_{235} = 0.99 \pm 0.02$, which is compatible with our r_{235} at less than 1σ . Our analysis also confirms the results on the value of $\sigma_{f,239}$ of Refs. [24–27], which assumed the absence of neutrino

oscillations, indicating that it is compatible with the theoretical prediction.

Let us now consider the 235+238+239 analysis in which also r_{238} is free. Figure 6 shows the allowed regions in the r_{235} - r_{239} , r_{238} - r_{239} , and r_{235} - r_{238} planes and the marginal $\Delta\chi^2$'s. From the figure and from Table I, one can see that the best-fit value of r_{238} is rather small, but the uncertainty of r_{238} is large. The small best-fit value of r_{238} pushes the best-fit values of r_{235} and r_{239} to values that are larger than those obtained in the 235+239 analysis. However, we have a compatibility within the 1σ uncertainty of the values of $\sigma_{f,235}$ and $\sigma_{f,239}$ obtained in the 235+239 and 235+238+239 analyses. In particular, as one can see from the marginal $\Delta\chi^2$ in Fig. 6(d), in the 235+238+239 analysis the theoretical value of $\sigma_{f,235}$ is disfavored at about 2σ . This result is less strong than the one found in the 235+239 case, where the theoretical value is disfavored at more than 3σ (see the marginal $\Delta\chi^2$ in Fig. 5), but it is still a significant finding.

For the ^{238}U antineutrino flux we find a relatively strong suppression ($r_{238} = 0.76_{-0.16}^{+0.15}$) but the uncertainty is large and the theoretical flux calculated in Ref. [11] is allowed at less than 2σ . A similar suppression of the ^{238}U antineutrino flux with a large uncertainty was found in Ref. [27] assuming the absence of neutrino oscillations. Let us remind that the ^{238}U antineutrino flux is the only one that was calculated in Ref. [11] “ab initio” using the nuclear databases. The corresponding β spectrum was measured afterwards in Ref. [85]. The resulting converted ν_e spectrum is larger than the calculated spectrum for $E_\nu \lesssim 3.5 \text{ MeV}$ and smaller for $4 \text{ MeV} \lesssim E_\nu \lesssim 6.5 \text{ MeV}$, albeit with large uncertainties (see Fig. 2 of Ref. [85]).

In our analysis we multiply the predicted rate of the GALLEX and SAGE experiment by the free coefficients η_G and η_S , respectively, which are the corrections to the detector efficiencies needed to fit the Gallium data in the MI ν_e Dis fit. The best-fit values and uncertainties of η_G and η_S are given in Table I. Figure 7 shows the allowed regions in the η_G - η_S plane and the marginal $\Delta\chi^2$'s. One can see that η_G and η_S are practically uncorrelated and the fit indicates that they are smaller than one, but the uncertainties are large. Hence, we cannot make a definite conclusion about the efficiencies of the GALLEX and SAGE detectors, but we think that it would be appropriate to take into account their uncertainties in the analysis of the GALLEX and SAGE solar neutrino data.

V. CONCLUSIONS

In this paper we have considered the new model-independent indications in favor of short-baseline $\bar{\nu}_e$ oscillations found in the DANSS experiment [36] and we have shown that they reinforce the model-independent indication in favor of short-baseline $\bar{\nu}_e$ oscillations found in the late 2016 in the NEOS experiment [23]. In the framework of 3+1 active-sterile neutrino mixing, the combined analysis of the DANSS and NEOS spectral ratios con-

strain at 2σ the two mixing parameters $\sin^2 2\vartheta_{ee}$ and Δm_{41}^2 to a narrow- Δm_{41}^2 island at $\Delta m_{41}^2 \simeq 1.3 \text{ eV}^2$, with $\sin^2 2\vartheta_{ee} = 0.049 \pm 0.023$ (2σ). If we consider the 3σ allowed regions, there are also two islands at $\Delta m_{41}^2 \simeq 0.4 \text{ eV}^2$ and $\Delta m_{41}^2 \simeq 2.5 \text{ eV}^2$. The statistical significance of the model-independent NEOS+DANSS indication in favor of short-baseline $\bar{\nu}_e$ oscillations is of 3.7σ .

We have shown that the DANSS and NEOS indication of short-baseline $\bar{\nu}_e$ oscillations is in tension with the reactor anomaly and with the Gallium anomaly. However, since the oscillation parameters are determined in a model-independent way by the NEOS and DANSS data, it is possible to analyze the data on the reactor and Gallium anomaly in a model-independent way, considering as free the main reactor antineutrino fluxes and the efficiencies of the GALLEX and SAGE detectors. We presented the results of two analyses of this type: one with free ^{235}U and ^{239}Pu fluxes and one in which also the ^{238}U is free. In these global model-independent analyses of short-baseline ν_e and $\bar{\nu}_e$ disappearance data we took into account also other data which constrain neutrino oscillations in a model-independent way: the Bugey-3 spectral ratio [59] and the ratio of the KARMEN [60] and LSND [61] $\nu_e + ^{12}\text{C} \rightarrow ^{12}\text{N}_{\text{g.s.}} + e^-$ scattering data. We

found that the strong constraints on short-baseline neutrino oscillations obtained from the DANSS and NEOS spectral ratios persist in the global model-independent analyses and allow us to obtain simultaneous information on neutrino oscillations, on the reactor antineutrino fluxes and on the efficiencies of the Gallium detectors. In particular, we confirm the indication in favor of the need for a recalculation of the ^{235}U cross sections per fission found in Refs. [24–27] assuming the absence of neutrino oscillations.

ACKNOWLEDGMENTS

The work of S.G. is supported by the Spanish grants FPA2017-85216-P, SEV-2014-0398 (MINECO), PROMETEOII/2014/084 (Generalitat Valenciana), and has received funding from the European Union’s Horizon 2020 research and innovation programme under the Marie Skłodowska-Curie grant agreement No 796941. The work of Y.F.L. is supported in part by the National Natural Science Foundation of China under Grant No. 11305193, by the Strategic Priority Research Program of the Chinese Academy of Sciences under Grant No. XDA10010100, and the CAS Center for Excellence in Particle Physics (CCEPP).

-
- [1] G. Mention *et al.*, Phys. Rev. **D83**, 073006 (2011), arXiv:1101.2755 [hep-ex].
- [2] J. N. Abdurashitov *et al.* (SAGE), Phys. Rev. **C73**, 045805 (2006), nucl-ex/0512041.
- [3] M. Laveder, Nucl. Phys. Proc. Suppl. **168**, 344 (2007).
- [4] C. Giunti and M. Laveder, Mod. Phys. Lett. **A22**, 2499 (2007), hep-ph/0610352.
- [5] M. A. Acero, C. Giunti, and M. Laveder, Phys. Rev. **D78**, 073009 (2008), arXiv:0711.4222 [hep-ph].
- [6] C. Giunti and M. Laveder, Phys. Rev. **D80**, 013005 (2009), arXiv:0902.1992 [hep-ph].
- [7] C. Giunti and M. Laveder, Phys. Rev. **C83**, 065504 (2011), arXiv:1006.3244 [hep-ph].
- [8] C. Giunti, M. Laveder, Y. Li, Q. Liu, and H. Long, Phys. Rev. **D86**, 113014 (2012), arXiv:1210.5715 [hep-ph].
- [9] S. Gariazzo, C. Giunti, M. Laveder, and Y. Li, JHEP **1706**, 135 (2017), arXiv:1703.00860 [hep-ph].
- [10] M. Dentler, A. Hernandez-Cabezudo, J. Kopp, M. Maltoni, and T. Schwetz, JHEP **1711**, 099 (2017), arXiv:1709.04294 [hep-ph].
- [11] T. A. Mueller *et al.*, Phys. Rev. **C83**, 054615 (2011), arXiv:1101.2663 [hep-ex].
- [12] P. Huber, Phys. Rev. **C84**, 024617 (2011), arXiv:1106.0687 [hep-ph].
- [13] P. Vogel, G. K. Schenter, F. M. Mann, and R. E. Schenter, Phys. Rev. **C24**, 1543 (1981).
- [14] K. Schreckenbach, G. Colvin, W. Gelletly, and F. Von Feilitzsch, Phys. Lett. **B160**, 325 (1985).
- [15] A. A. Hahn *et al.*, Phys. Lett. **B218**, 365 (1989).
- [16] S. Gariazzo, C. Giunti, M. Laveder, Y. Li, and E. Zavanin, J. Phys. **G43**, 033001 (2016), arXiv:1507.08204 [hep-ph].
- [17] P. Huber, Nucl. Phys. **B908**, 268 (2016), arXiv:1602.01499 [hep-ph].
- [18] A. C. Hayes and P. Vogel, Ann.Rev.Nucl.Part.Sci. **66**, 219 (2016), arXiv:1605.02047 [hep-ph].
- [19] S.-H. Seo (RENO), AIP Conf. Proc. **1666**, 080002 (2015), arXiv:1410.7987 [hep-ex].
- [20] J. Choi *et al.* (RENO), Phys. Rev. Lett. **116**, 211801 (2016), arXiv:1511.05849 [hep-ex].
- [21] Y. Abe *et al.* (Double Chooz), JHEP **10**, 086 (2014), [Erratum: JHEP 02, 074 (2015)], arXiv:1406.7763 [hep-ex].
- [22] F. An *et al.* (Daya Bay), Chin.Phys. **C41**, 013002 (2017), arXiv:1607.05378 [hep-ex].
- [23] Y. Ko *et al.* (NEOS), Phys.Rev.Lett. **118**, 121802 (2017), arXiv:1610.05134 [hep-ex].
- [24] F. P. An *et al.* (Daya Bay), Phys.Rev.Lett. **118**, 251801 (2017), arXiv:1704.01082 [physics].
- [25] C. Giunti, Phys.Rev. **D96**, 033005 (2017), arXiv:1704.02276 [hep-ph].
- [26] C. Giunti, X. P. Ji, M. Laveder, Y. F. Li, and B. R. Littlejohn, JHEP **1710**, 143 (2017), arXiv:1708.01133 [hep-ph].
- [27] Y. Gebre, B. R. Littlejohn, and P. T. Surukuchi, Phys.Rev. **D97**, 013003 (2018), arXiv:1709.10051 [hep-ph].
- [28] X. Qian and J.-C. Peng, arXiv:1801.05386 [hep-ex].
- [29] P. Anselmann *et al.* (GALLEX), Phys. Lett. **B342**, 440 (1995).
- [30] W. Hampel *et al.* (GALLEX), Phys. Lett. **B420**, 114 (1998).

- [31] F. Kaether, W. Hampel, G. Heusser, J. Kiko, and T. Kirsten, *Phys. Lett.* **B685**, 47 (2010), arXiv:1001.2731 [hep-ex].
- [32] J. N. Abdurashitov *et al.* (SAGE), *Phys. Rev. Lett.* **77**, 4708 (1996).
- [33] J. N. Abdurashitov *et al.* (SAGE), *Phys. Rev.* **C59**, 2246 (1999), hep-ph/9803418.
- [34] J. N. Abdurashitov *et al.* (SAGE), *Phys. Rev.* **C80**, 015807 (2009), arXiv:0901.2200 [nucl-ex].
- [35] D. Frekers, H. Ejiri, H. Akimune, T. Adachi, B. Bilgier, *et al.*, *Phys. Lett.* **B706**, 134 (2011).
- [36] M. Danilov, (2017), talk presented at Solvay Workshop 'Beyond the Standard model with Neutrinos and Nuclear Physics', 29 November - 1 December 2017, Brussels, Belgium.
- [37] I. Esteban, M. C. Gonzalez-Garcia, M. Maltoni, I. Martinez-Soler, and T. Schwetz, *JHEP* **1701**, 087 (2017), arXiv:1611.01514 [hep-ph].
- [38] F. Capozzi *et al.*, *Phys.Rev.* **D95**, 096014 (2017), arXiv:1703.04471 [hep-ph].
- [39] P. F. de Salas, D. V. Forero, C. A. Ternes, M. Tortola, and J. W. F. Valle, arXiv:1708.01186 [hep-ph].
- [40] S. M. Bilenky, C. Giunti, and W. Grimus, *Eur. Phys. J.* **C1**, 247 (1998), hep-ph/9607372.
- [41] C. Athanassopoulos *et al.* (LSND), *Phys. Rev. Lett.* **75**, 2650 (1995), nucl-ex/9504002.
- [42] A. Aguilar *et al.* (LSND), *Phys. Rev.* **D64**, 112007 (2001), hep-ex/0104049.
- [43] P. Adamson *et al.* (MINOS), arXiv:1710.06488 [hep-ex].
- [44] N. Okada and O. Yasuda, *Int. J. Mod. Phys.* **A12**, 3669 (1997), hep-ph/9606411.
- [45] J. Kopp, M. Maltoni, and T. Schwetz, *Phys. Rev. Lett.* **107**, 091801 (2011), arXiv:1103.4570 [hep-ph].
- [46] C. Giunti and M. Laveder, *Phys. Rev.* **D84**, 073008 (2011), arXiv:1107.1452 [hep-ph].
- [47] C. Giunti and M. Laveder, *Phys. Rev.* **D84**, 093006 (2011), arXiv:1109.4033 [hep-ph].
- [48] C. Giunti and M. Laveder, *Phys. Lett.* **B706**, 200 (2011), arXiv:1111.1069 [hep-ph].
- [49] J. Conrad, C. Ignarra, G. Karagiorgi, M. Shaevitz, and J. Spitz, *Adv.High Energy Phys.* **2013**, 163897 (2013), arXiv:1207.4765 [hep-ex].
- [50] M. Archidiacono, N. Fornengo, C. Giunti, and A. Melchiorri, *Phys. Rev.* **D86**, 065028 (2012), arXiv:1207.6515 [astro-ph].
- [51] M. Archidiacono, N. Fornengo, C. Giunti, S. Hannestad, and A. Melchiorri, *Phys. Rev.* **D87**, 125034 (2013), arXiv:1302.6720 [astro-ph].
- [52] J. Kopp, P. A. N. Machado, M. Maltoni, and T. Schwetz, *JHEP* **1305**, 050 (2013), arXiv:1303.3011 [hep-ph].
- [53] C. Giunti, M. Laveder, Y. Li, and H. Long, *Phys. Rev.* **D88**, 073008 (2013), arXiv:1308.5288 [hep-ph].
- [54] L. Aliaga *et al.* (MINERvA), *Phys. Rev.* **D94**, 092005 (2016), arXiv:1607.00704 [physics].
- [55] R. Acciarri *et al.* (MicroBooNE, LAr1-ND, ICARUS-WA104), arXiv:1503.01520 [physics].
- [56] S. Ajimura *et al.*, arXiv:1705.08629 [physics].
- [57] M. Maltoni and T. Schwetz, *Phys. Rev.* **D68**, 033020 (2003), hep-ph/0304176.
- [58] C. Giunti, M. Laveder, Y. Li, and H. Long, *Phys. Rev.* **D87**, 013004 (2013), arXiv:1212.3805 [hep-ph].
- [59] B. Achkar *et al.* (Bugey), *Nucl. Phys.* **B434**, 503 (1995).
- [60] B. Armbruster *et al.* (KARMEN), *Phys. Rev.* **C57**, 3414 (1998), hep-ex/9801007.
- [61] L. B. Auerbach *et al.* (LSND), *Phys. Rev.* **C64**, 065501 (2001), hep-ex/0105068.
- [62] J. Conrad and M. Shaevitz, *Phys. Rev.* **D85**, 013017 (2012), arXiv:1106.5552 [hep-ex].
- [63] Y. Declais *et al.* (Bugey), *Phys. Lett.* **B338**, 383 (1994).
- [64] A. Kuvshinnikov, L. Mikaelyan, S. Nikolaev, M. Skorkhvatov, and A. Etenko, *JETP Lett.* **54**, 253 (1991).
- [65] G. Zacek *et al.* (CalTech-SIN-TUM), *Phys. Rev.* **D34**, 2621 (1986).
- [66] H. Kwon *et al.*, *Phys. Rev.* **D24**, 1097 (1981).
- [67] A. Hoummada, S. Lazrak Mikou, G. Bagieu, J. Cavaignac, and D. Holm Koang, *Applied Radiation and Isotopes* **46**, 449 (1995).
- [68] G. S. Vidyakin *et al.* (Krasnoyarsk), *Sov. Phys. JETP* **66**, 243 (1987).
- [69] G. S. Vidyakin *et al.* (Krasnoyarsk), *Sov. Phys. JETP* **71**, 424 (1990).
- [70] G. S. Vidyakin *et al.* (Krasnoyarsk), *JETP Lett.* **59**, 390 (1994).
- [71] A. I. Afonin *et al.*, *Sov. Phys. JETP* **67**, 213 (1988).
- [72] Z. D. Greenwood *et al.*, *Phys. Rev.* **D53**, 6054 (1996).
- [73] G. Boireau *et al.* (NUCIFER), *Phys. Rev.* **D93**, 112006 (2016), arXiv:1509.05610 [physics].
- [74] M. Apollonio *et al.* (CHOOZ), *Eur. Phys. J.* **C27**, 331 (2003), hep-ex/0301017.
- [75] F. Boehm *et al.* (Palo Verde), *Phys. Rev.* **D64**, 112001 (2001), hep-ex/0107009.
- [76] H. Seo, (2016), talk presented at AAP 2016, Applied Antineutrino Physics, 1-2 December 2016, Liverpool, UK.
- [77] Double Chooz Collaboration, Private Communication.
- [78] J. Ashenfelter *et al.* (PROSPECT), *J. Phys.* **G43**, 113001 (2016), arXiv:1512.02202 [physics].
- [79] I. Michiels (SoLid), arXiv:1605.00215 [physics].
- [80] L. Manzanillas (STEREO), *PoS NOW2016*, 033 (2017), arXiv:1702.02498 [physics.ins-det].
- [81] G. Bellini *et al.* (Borexino), *JHEP* **1308**, 038 (2013), arXiv:1304.7721 [physics].
- [82] G. Drexlin, (2016), talk presented at NOW 2016, 4-11 September 2016, Otranto, Lecce, Italy.
- [83] M. Abs *et al.*, arXiv:1511.05130 [physics].
- [84] E. Ciuffoli, J. Evslin, and F. Zhao, *JHEP* **01**, 004 (2016), arXiv:1509.03494 [hep-ph].
- [85] N. Haag, A. Gutlein, M. Hofmann, L. Oberauer, W. Potzel, *et al.*, *Phys. Rev. Lett.* **112**, 122501 (2014), arXiv:1312.5601 [nucl-ex].